Archives of Materials Science and Engineering

Volume 42
Issue 1
March 2010
Pages 37-44

International Scientific Journal
published monthly by the
World Academy of Materials
and Manufacturing Engineering

# Weldability of 440 MPa galvanized steel with inverter DC resistance spot welding process

**I.S. Hwang [a], H.J. Yoon [b], M.J. Kang [a] , D.C. Kim [a,*]**

[a] Advanced Joining Technology Team, Korea Institute of Industrial Technology,
7-47 Songdo-Dong, Incheon, South Korea
[b] Department of Mechanical Engineering, Hanyang University,
17 Haengdang-Dong, Seoul, South Korea
* Corresponding author: E-mail address: dckim@kitech.re.kr

Received 13.01.2010; published in revised form 01.03.2010

## ABSTRACT

**Purpose:** This paper comparatively analyzes resistance spot weldability depending on whether or not 440 MPa-grade steel is galvanized at inverter DC spot welding.

**Design/methodology/approach:** To compare the resistance spot weldability depending on whether or not the steel is galvanized, an inverter DC welding system was designed. Then, using this system, both tensile strength testing and macro-section testing were conducted on SPRC440 (uncoated steel) and SGARC440 (galvanized steel), and weldability was evaluated. Suitable welding conditions were calculated using the resistance spot welding variables such as electrode force, welding time and lobe diagram on the welding current. The low limit of the lobe diagram was set to the low limit of the tensile strength of 440 MPa-grade steel while the high limit was set depending on whether or not expulsion was detected.

**Findings:** Compared to uncoated steel, galvanized steel had lower suitable welding current conditions and a narrower lobe diagram.

**Research limitations/implications:** This paper compared resistance spot weldability and lobe diagram depending on whether or not 440 MPa-grade steel is galvanized.

**Practical implications:** This paper confirms the weldability of galvanized steel by comparing resistance spot weldability depending on whether or not steel is galvanized.

**Originality/value:** For analysis of resistance spot weldability depending on whether or not steel is galvanized, weldability was compared between SPRC440 (uncoated steel) and SGARC440 (galvanized steel) under the same welding conditions. As a result, compared to uncoated steel, galvanized steel had lower suitable welding current conditions and a narrower lobe diagram.

**Keywords:** Resistance spot welding; SPRC440; SGARC440; Inverter DC spot welding system; Lobe diagram

**Reference to this paper should be given in the following way:**

I.S. Hwang, H.J. Yoon, M.J. Kang, D.C. Kim, Weldability of 440 MPa galvanized steel with inverter DC resistance spot welding process, Archives of Materials Science and Engineering 42/1 (2010) 37-44.

MATERIALS MANUFACTURING AND PROCESSING

## 1. Introduction

Resistance spot welding is a process that uses resistance Joule heat which occurs when a high current is applied with contact resistance that exists between metals and their specific resistance. This welding process is widely used in assembling steel sheets such as car bodies. Two welding current methods - SCR AC and inverter DC – were used. The former has been used in assembling car bodies while the inverter DC has been widely used in the welding of aluminum, aircraft parts and trains. In general, unlike SCR AC, welding with low current is possible with a wide welding range using the inverter DC e. Furthermore, the inverter DC has the advantage of low electrode wear.

In the car industry, galvanized steel sheets with great corrosion resistance and durability have been most commonly used. However, problems in suitable welding conditions and electrode wear have been observed during resistance welding. The former has the problem of a high current with narrow suitable welding conditions while electrode wear can shorten the life of an electrode from continuous welding after it has been contaminated by zinc at a low melting range. To solve these problems, it is necessary to decrease electrode damage by supplying the current in a stable manner and shortening welding time through high-speed control. However, these functions are impossible for SCR AC. For this reason, the inverter DC is preferred.

In this paper, the inverter DC welding system was designed to evaluate the weldability of 440 MPa-grade galvanized steel. To stabilize welding power, furthermore, constant current control was realized after designing the PI controller. In terms of welding materials, uncoated steel sheets - SPRC440 (1.4 mmt) and galvanized steel sheets - SGARC440 (1.4 mmt) – were used. Then, the weldability of galvanized steel was compared through tensile strength testing and macro-section testing. In addition, lobe diagrams were compared.

## 2. Resistance spot welding system

### 2.1. Inverter DC welding system

In general, the inverter DC welding system uses 220-660V, 3-phase power. As shown in Fig. 1, the 3-phase power gets smoothened DC current through a DC link-called capacitor after rectification using 6 diodes or a thyristor. The DC link acts as both filter and stub in the circuit. The voltage created in the DC link acts as the inverter power. After configuring IGBT to the H-bridge shape, the inverter creates single-phase voltage. Here, frequency, which is higher than the one (60 Hz) used in the SCR AC welding system, is used. In general, 1 kHz, called MFDC, is used. Due to the increase in switching frequency, the size of the transformer for creation of a large current in the resistance spot welding system decreases. The welding power with increased frequency amplifies current through a transformer and reduces voltage. The power amplified in the secondary transformer passes through a reactor and is transformed into direct current after rectification using a diode.

In the SCR AC welding system, sine-wave voltage is turned on using a switching device just like the thyristor. Therefore, voltage variation at the turn-on point continues until the secondary voltage. In the inverter DC welding system, on the contrary, a certain level of fixed voltage is used at the DC link and delivered to a transformer. Therefore, it is quite different in terms of the control method. In the inverter DC welding system, the turn-on/off time of the IGBT is decided based on the Pulse Width Modulation (PWM) control method.

### 2.2. Development of welding system

In this paper, an inverter DC welding system was designed for the welding test. To control high-speed current, ultra-fast MCU-TMS320LF2812 was used. In addition, the change in weldability caused by setup errors during the welding test has been minimized by digitalizing the welding time setting. Fig. 2 illustrates the configuration of the inverter DC welding system while Table 1 describes the welding specifications. Fig. 3 shows the current waveforms of the internally designed inverter DC welding system. Constant DC current is observed in the waveforms.

Table 1.
Specification of developed welding system

| Parameter | Inverter DC welding system |
|---|---|
| Input voltage | 440 VAC |
| Frequency | 1 kHz |
| Maximum current | 35 kA |
| Maximum electrode force | 500 $kg_f/cm^2$ |

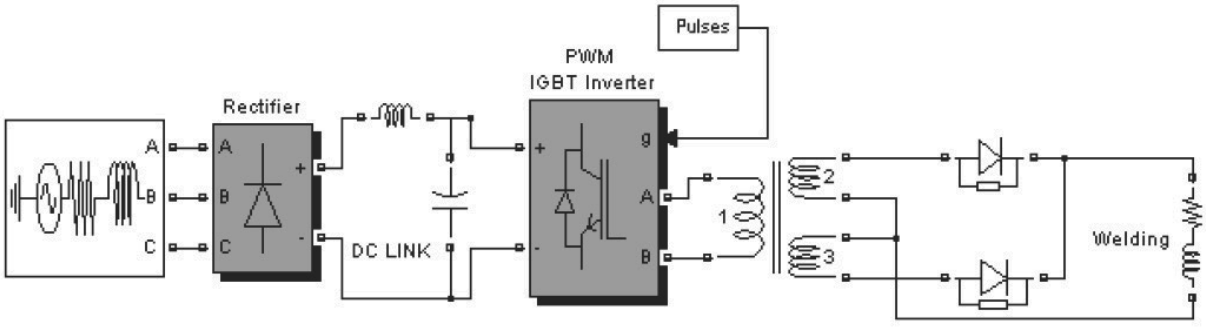


Fig. 1. Inverter DC welding system

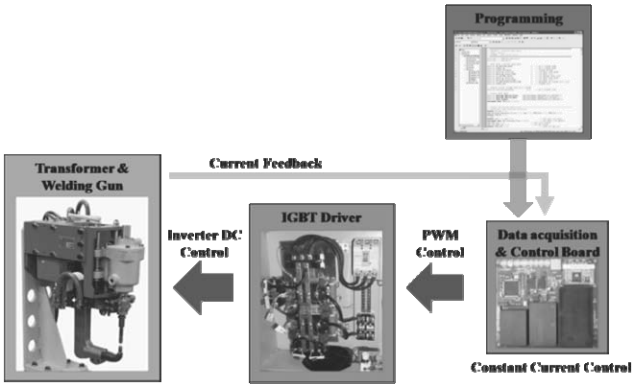


Fig. 2. Structure of developed welding system

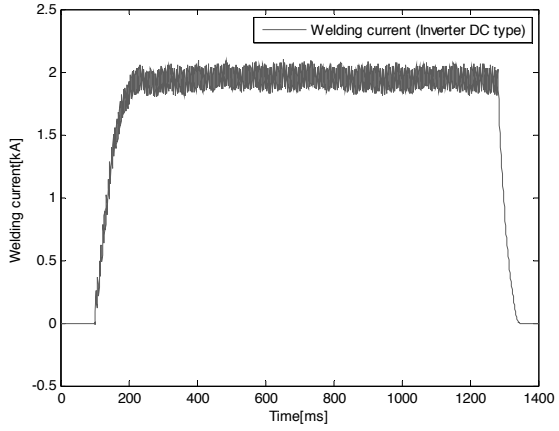


Fig. 3. Current waveform of developed welding system

## 3. Design of constant current control

### 3.1. PI control

PI control is the most common method. PI control refers to a control method using Proportional Gain (P) and Integral Gain (I). Here, proportional gain refers to a control counter proportionate to the size of the error while the integral gain refers to a control counter which is acquired after integrating errors. Fig. 4 shows the control structure of PI control.

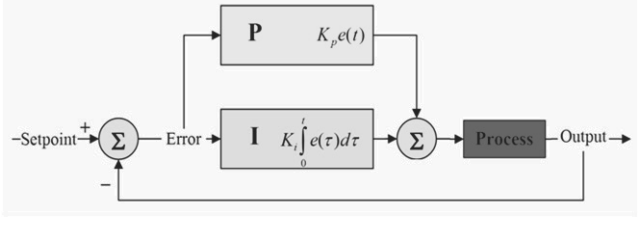


Fig. 4. PI control structure

Due to its ease of use, PI control has been widely used in controlling industrial equipment. It accelerates system response which has been slowed by transient response by reducing steady-state errors.

### 3.2. Design of PI controller

In this paper, constant current control was designed using the PI controller. constant current control refers to a control to prevent the ripple of current by load variation. After modification of 'P' and 'I' control counters through a repetitive test, the static current PI controller was designed. Fig. 5 illustrates current signal waveforms before and after constant current control. As shown in this figure, welding current ripple was observed over load variation before static current control. Furthermore, the current was low because of the load. On the contrary, constant current was observed in static current waveforms regardless of load variation.

a)

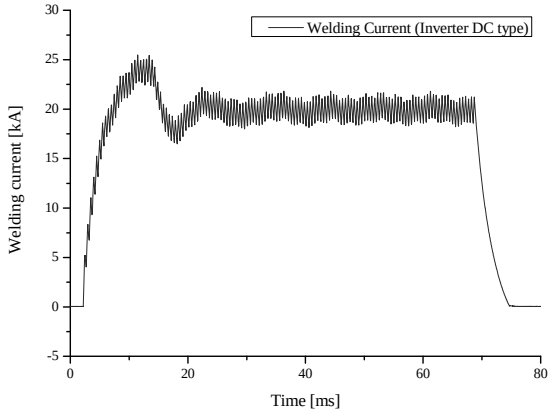


b)

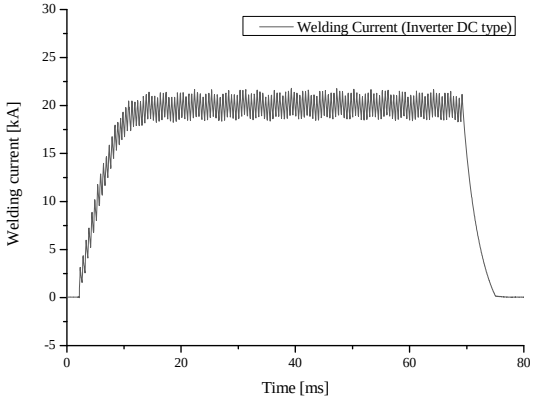


Fig. 5. Current waveform with current control: a) None constant current control, b) Constant current control

# 4. Experiments

## 4.1. Experiments setup

To assess weldability of 440 MPa-grade galvanized steel sheets, welding conditions were set through preceding experiments because they can vary depending on coating conditions even though the same steel is used. In this paper, whether or not torsion and expulsion occurred was tested through the preceding experiments. Then, suitable welding conditions were set. Table 2 and show welding conditions by steel sheet. In SPRC440, welding current, welding time and electrode force were set to level 7 (4-10 kA with 1 kA interval), level 5 (4-12 cycles with 2 cycle interval) and level 3 (200-300 $kg_f/cm^2$ with 100 $kg_f/cm^2$), respectively. In SGARC440, welding current, welding time and electrode force were set to level 8 (4-11 kA with 1 kA interval), level 5 (4-12 cycles with 2 cycle interval) and level 3 (200-300 $kg_f/cm^2$ with 100 $kg_f/cm^2$), respectively.

Table 2.
Experiments setup

| | |
|---|---|
| Base metal | SPRC440, 1.4 mmt |
| Current | 4, 5, 6, 7, 8, 9, 10 [kA] |
| Welding Time | 4, 6, 8, 10, 12 [cycle] |
| Electrode Force | 200, 300, 400 [$kg_f/cm^2$] |
| Base metal | SGARC440, 1.4 mmt |
| Current | 4, 5, 6, 7, 8, 9, 10, 11 [kA] |
| Welding Time | 4, 6, 8, 10, 12 [cycle] |
| Electrode Force | 200, 300, 400 [$kg_f/cm^2$] |

Fig. 6 shows the dimensions of welding test specimen. For a welding electrode, dome-type, chrome-copper electrode has been used. Fig. 7 illustrates the dimension of welding electrode while Table 3 describes the characteristics.

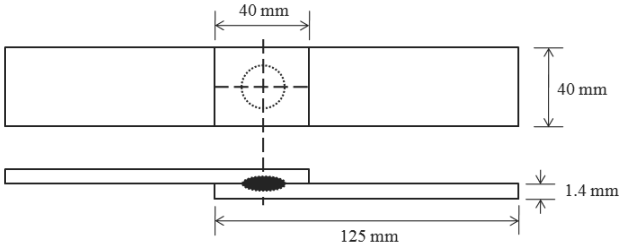


Fig. 6. Schematic illustration of weld specimen

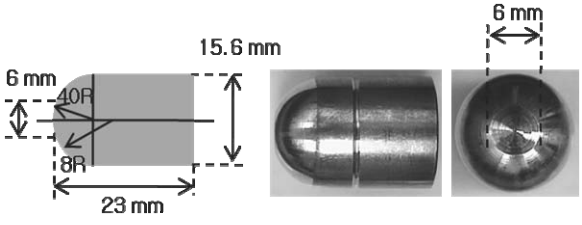


Fig. 7. Schematic illustration and shape of electrode

Table 3.
Characteristic of electrode

| | |
|---|---|
| Chemical composition | Cr(0.5~1%), Cu(Bal.) |
| Hardness(HRB) | 72 |
| Electric conductivity | 75% |
| Tensile strength | 42 $kg/mm^2$ |
| Vicat softening temperature | 460°C |

## 4.2. Evaluation of weldabillity

According to welding conditions, welding experiments were conducted to evaluate weldability. To evaluate weldability, tensile strength testing and macro-section testing were carried out. For the tensile strength test, Shimadzu Corporation's Universal Tester, which can cover up to 30 tons of loads, was used. For the macro-section test, on the other hand, a section of the test specimen is processed and etched using a strong alkali solution. Then, the nugget size was measured.

## 4.3. Lobe diagram

A lobe diagram is a graph indicating the evaluation of the resistance spot weldability that shows an appropriate welding range by changing two factors while fixing one factor of resistance spot welding such as electrode force, welding time, and welding current. In this study, the welding current–time lobe diagram was used with the electrode force fixed. The horizontal axis was set as the welding current, and the longitudinal axis as the welding time. Fig. 8 shows an example of the welding current-time lobe diagram. The low limit, the left boundary line of the lobe diagram, was set to 8279 N (the permission tensile strength) while the high limit, the right boundary line, was set depending on whether or not expulsion occurred.

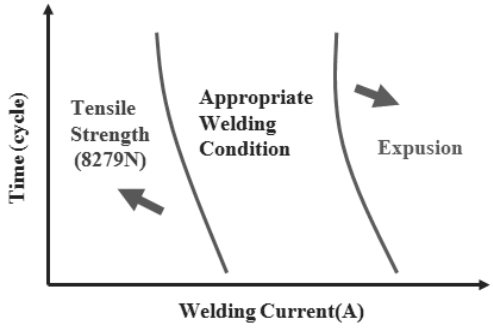


Fig. 8. Current-time lobe diagram

# 5. Results and discussion

## 5.1. Tensile strength test

The Figures (from Fig. 9 to Fig. 11) show the results of the tensile strength test on 440 MPa-grade galvanized steel. It was

confirmed that tensile strength increased with the increase in welding current and time under all electrode force conditions. When expulsion occurred, no change was observed over the welding time despite high tensile strength because an excessive increase in heat input made melting unstable, drive melt sources sprung forth and induced inconsistent melting parts in terms of size.

Fig. 9 indicates the tensile strength graph at 200 $kg_f/cm^2$ of electrode force. According to the graph, the increase in tensile strength was observed as the current increased. When current conditions were compared, however, SGARC440 was relatively higher. Furthermore, the galvanized steel sheet was lower than the uncoated steel in terms of tensile strength despite higher current conditions.

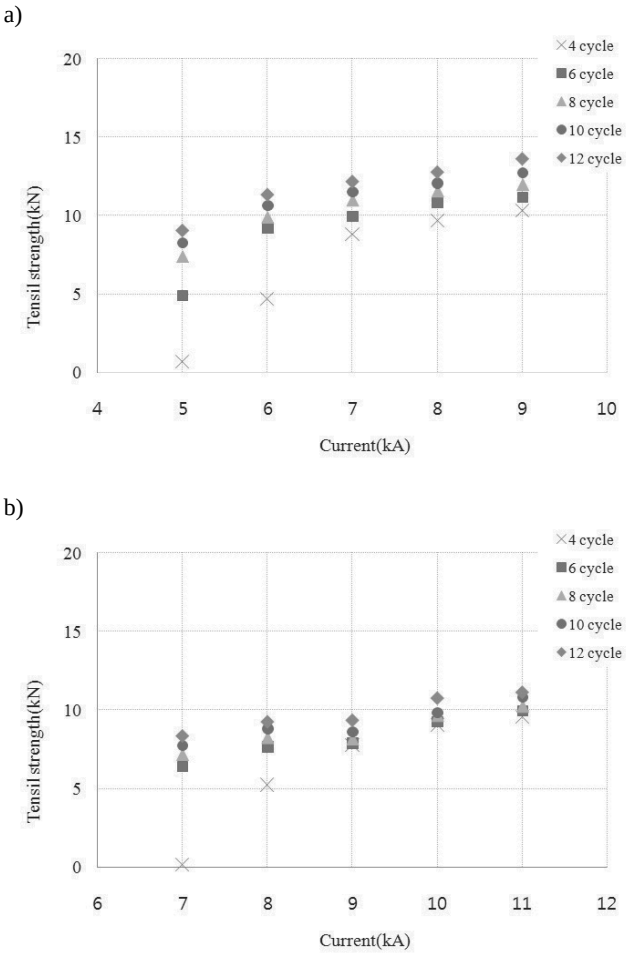


Fig. 9. Tensile strength of electrode force 200 $kg_f/cm^2$: a) SPRC440, 1.4 mmt, b) SGARC440, 1.4 mmt

The same characteristics were observed in Fig. 10 and Fig. 11 because zinc is higher than iron in terms of electric conductivity. In the beginning of welding, zinc melts prior to iron due to its lower melting point. Zinc remains partially on the surface of steel after partially evaporating. Because of this zinc, current flows into the edge of the melting part, failing to concentrate on it. As a result, galvanized steel density is lower than uncoated steel in terms of current density at the melting part. Therefore, a higher current is required for resistance spot welding.

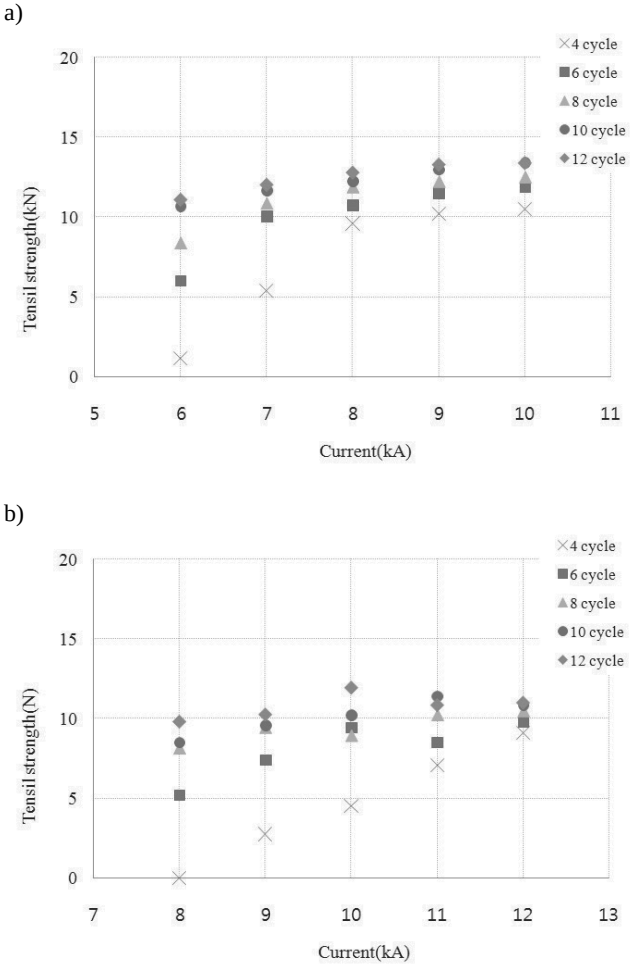


Fig. 10. Tensile strength of electrode force 300 $kg_f/cm^2$: a) SPRC440, 1.4 mmt, b) SGARC440, 1.4 mmt

Fig. 12 illustrates the results under the same conditions for an accurate comparison of tensile strength. A comparison has been made under 7 kA-8 cycle, 9 kA-8 cycle and 10 kA-8 cycle conditions when the electrode force was 200, 300 and 400 $kg_f/cm^2$, respectively. As shown in this figure, SPRC440, the uncoated steel sheet, showed higher tensile strength under the same current conditions. In other words, it was confirmed that a higher current should be applied to make the galvanized steel as strong as the uncoated steel in terms of tensile strength.

a)

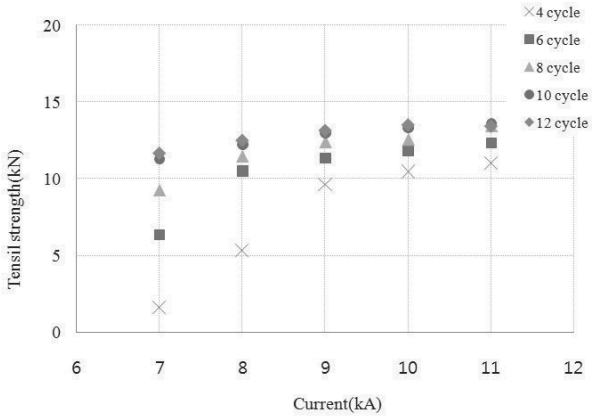


b)

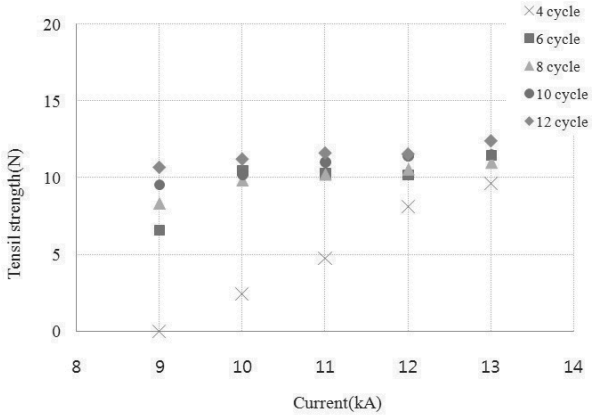


Fig. 11. Tensile strength of electrode force 400 $kg_f/cm^2$: a) SPRC440, 1.4 mmt, b) SGARC440, 1.4 mmt

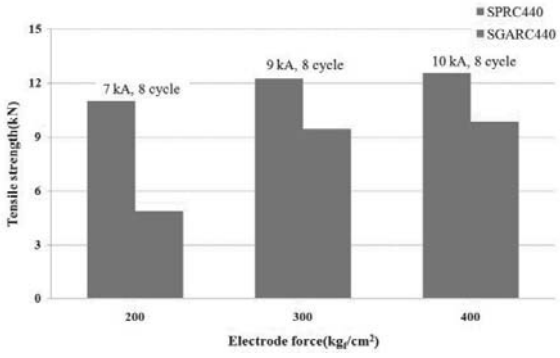


Fig. 12. Comparison of tensile strength by same conditions

## 5.2. Macro-section test

Fig. 13 shows the results under the same conditions for comparison of a nugget diameter. A comparison has been made under 7 kA-8 cycle, 9 kA-8 cycle and 10 kA-8 cycle conditions when electrode force was 200, 300 and 400 $kg_f/cm^2$, respectively.

When electrode force was 200 $kg_f/cm^2$, SPRC440 had greater nugget diameter (by 1 mm or more). When electrode force was 300 and 400 $kg_f/cm^2$, the uncoated steel produced larger nugget diameter with a minor difference because the current failed to concentrate on the melting part because of melting on the galvanized layer. Fig. 14 compares nugget diameters under the same conditions for easier understanding. As shown in this figure, nugget diameter is larger in SPRC440, uncoated steel.

a)

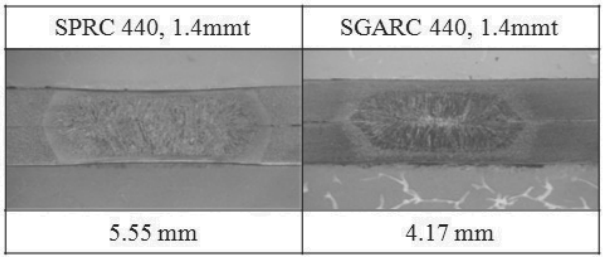


b)

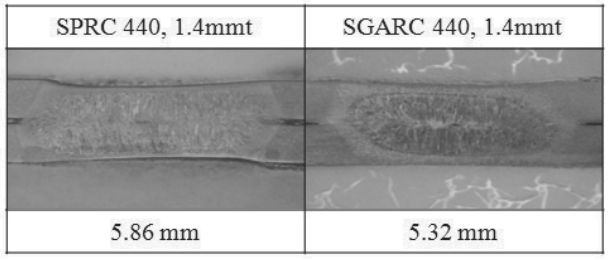


c)

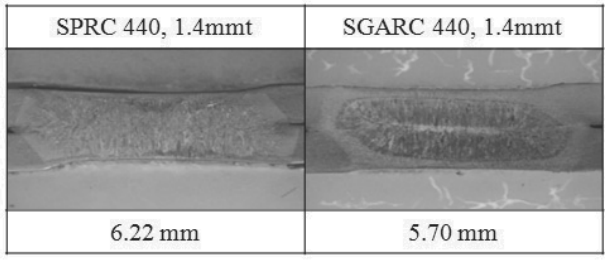


Fig. 13. Nugget image of same conditions: a) 9 kA, 8 cycle, 300 $kg_f/cm^2$, b) 9 kA, 8 cycle, 300 $kg_f/cm^2$, c) 10 kA, 8 cycle, 400 $kg_f/cm^2$

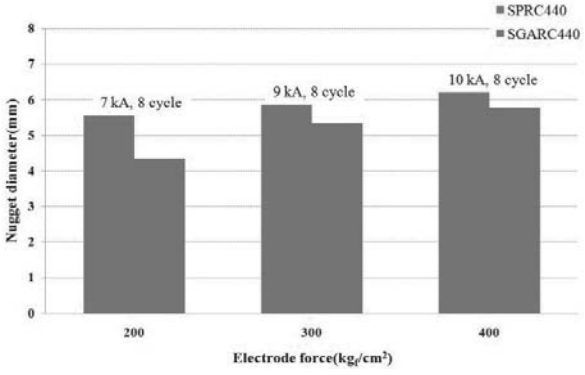


Fig. 14. Comparison of nugget diameter by same conditions

### 5.3. Evaluation of lobe diagram

The Figures (from Fig. 15 to Fig. 17) show the results of the lobe diagram depending on whether or not 440 MPa-grade steel is galvanized. For comparison of fracture shapes in addition to suitable welding conditions, a fracture shape was added to the lobe diagram. In the lobe diagram, round and diamond shapes are seen. The former represents an interfacial fracture while the latter stands for a plug fracture. Here, the interfacial fracture is a fracture in the melting part while the plug fracture is a base metal-broken fracture. In general, if a plug fracture occurs, it means that the melting part is stronger than the base metal with higher quality.

When electrode force was 200 $kg_f/cm^2$, SPRC440 (uncoated steel) was narrower than SGARC440 (galvanized steel) in terms of the shape of the lobe diagram. In terms of the size of scope of the lobe diagram, furthermore, SGARC440 was slightly greater than SPRC440. In terms of overall tensile strength, SPRC440 was greater than SGARC440 because of the decrease in current density after the melting of the galvanized layer and stable spread of heat input.

When electrode force was 300 $kg_f/cm^2$, SPRC440 (uncoated steel) was broader than SGARC440 (galvanized steel) in terms of the shape of the lobe diagram. This phenomenon became stronger as electrode force increased (400 $kg_f/cm^2$) because heat input was stable in uncoated steel sheets due to stable contact resistance at a certain level of electrode force. Under galvanized steel, however, heat input was dispersed by the melting of the coated layer.

a)

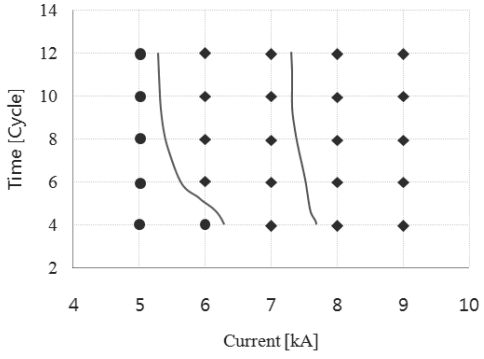


b)

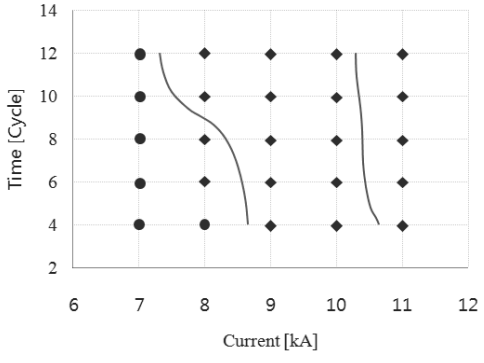


Fig. 15. Lobe diagram of electrode force 200 $kg_f/cm^2$: a) SPRC440, 1.4 mmt, b) SGARC440, 1.4 mmt

a)

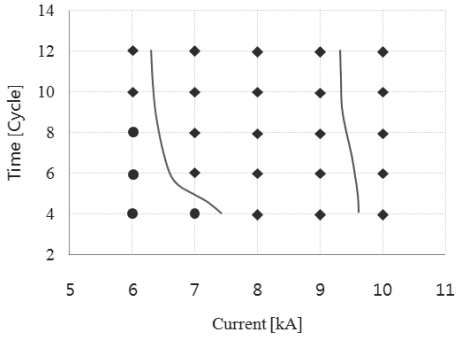


b)

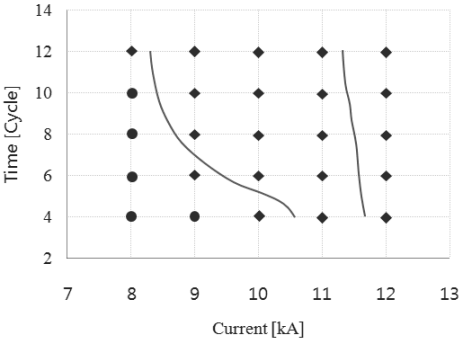


Fig. 16. Lobe diagram of electrode force 300 $kg_f/cm^2$: a) SPRC440, 1.4 mmt, b) SGARC440, 1.4mmt

a)

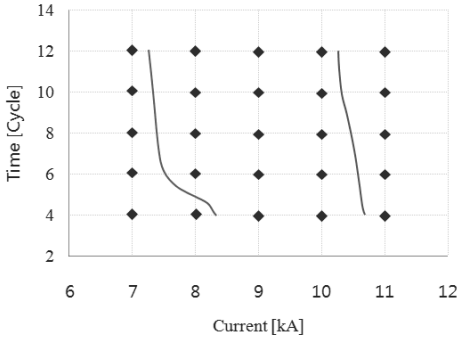


b)

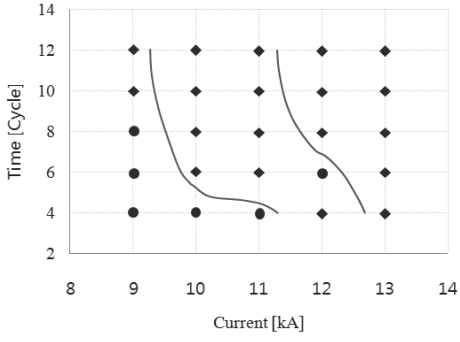


Fig. 17. Lobe diagram of electrode force 400 $kg_f/cm^2$: a) SPRC440, 1.4 mmt, b) SGARC440, 1.4 mmt

## 6. Conclusions

In this paper, an inverter DC welding system was designed to evaluate the weldability of 440 MPa-grade galvanized steel sheets. To stabilize welding power, furthermore, constant current control has been realized after designing the PI controller. In terms of welding materials, uncoated steel sheets - SPRC440 (1.4 mmt) and SGARC440 (1.4 mmt) – were used. Then, the weldability of galvanized steel was compared through the tensile strength test and macro-section test. In addition, lobe diagrams were compared. As a result, this paper has obtained the following conclusions:

1) Because of the decrease in current density after melting the galvanized layer, SGARC440 (galvanized steel) was lower than SPRC440 (uncoated steel) in terms of tensile strength under the same welding conditions;
2) Under the same conditions, SGARC440 was smaller and weaker than SPRC440 in terms of nugget diameter and tensile strength;
3) When electrode force was 200 $kg_f/cm^2$, SGARC440 was broader than SPRC440 in terms of the shape of the lobe diagram. When electrode force was 300 or 400 $kg_f/cm^2$, on the contrary, SGARC440 was narrower than SPRC440;
4) When heat input was unstable because of high contact resistance, an increase in current density caused by the melting of the coated layer eased the unstable conditions.

## References


[1] K.C. Kim, M.Y. Lee, T.J. Lim, Effect of Process Parameters of Heat Input Efficiency in Condenser Discharge Welding, Journal of KWS 5/1(1996) 3-5.

[2] H.S. Jang, S.B. Joe, Real-time Measurement of Power and Dynamic Resistance in Resistance Spot Welding, Journal of KWS (2003) 143-145.

[3] G. Mrówka-Nowotnik, J. Sieniawski, M. Wierzbińska, Intermetallic phase particles in 6082 aluminium, Archives of Materials Science and Engineering 28/2 (2007) 69-76.

[4] M. Kciuk, The structure, mechanical properties and corrosion resistance of aluminium $AlMg_1Si_1$ alloy, Journal of Achievements in Materials and Manufacturing Engineering 16 (2006) 51-56.

[5] J. Adamowski, M. Szkodo, FSW of aluminium alloy AW6082-T6, Journal of Achievements in Materials and Manufacturing Engineering 20 (2007) 403-406.

[6] J. Adamowski, C. Gambaro, E. Lertora, M. Ponte, M. Szkodo, Analysis of FSW welds made of aluminium alloy AW6082-T6, Archives of Materials Science and Engineering 28/8 (2007) 453-460.

[7] T.S. Kumar, V. Balasubramanian, M.Y. Sanavullah, Influences of pulsed current tungsten inert gas welding parameters on the tensile properties of AA 6061 aluminium alloy, Materials and Design 28 (2007) 2080-2092.

[8] E.A. Patrick, J.R. Auhl, T.S. Sun, Understanding the process mechanisms is Key to Reliable Resistance spot Welding Aluminum Auto Body Components, SAE paper 840291, 1984.

[9] G.L. Leone, B. Altshuller, Improvement on the Resistance Spot Weldability of Aluminum Body sheet, SAE paper 840292, 1984.

[10] W. Dilay, E.A. Rogala, E.J. Zubinski, Resistance welding aluminium for automotive production, SAE paper 77030, 1977.

[11] A.R. Krause, P.H. Thornton, R.G. Davies, Effect of Magnesium Content, on the Fatigue of Spot–Welded Aluminum Alloys, Proceedings of the Conference "Recent Developments in Light Metals", Torronto, Ontario, Canada, 1996, 305-314.

[12] B.M. Brown, A Comparison of AC and DC Resistance Welding of Automotive Steels, Welding Journal 66/1 (1987) 18-23.

[13] P.K.D.V. Yarlagadda, P. Praveen, V.K. Madasu, S. Rhee, Detection of short circuit in pulse gas metal arc welding process, Journal of Achievements in Materials and Manufacturing Engineering 24/1 (2007) 328-332.

[14] P. Praveen, M.J. Kang, P.K.D.V. Yarlagadda, Characterization of dynamic behaviour of short circuit in pulsed Gas Metal Arc Welding of aluminium, Journal of Achievements in Materials and Manufacturing Engineering 14 (2006) 75-82.

[15] H.L Sree, A. Soumitra, Spot Weldability of Advanced High strength Steels using AC and MFDC power sources, Proceedings of the 11th Sheet Metal Welding Conference, Detroit, Michigan, 2004, 11-14.

[16] H. Yamamoto, Recent advances in inverter controlled arc welding power sources and their application, Journal of Japan Welding Society 58 (1989) 273.